Utilizing pineapple peel crosslinked chitosan as an eco-friendly biosorbent for heavy metal removal: A circular economy perspective

Nguyen My Linh[*]

Use your smartphone to scan this QR code and download this article

Faculty of Chemical and Food Technology, Ho Chi Minh City University of Technology and Education, HCMC, Vietnam

Correspondence

Nguyen My Linh, Faculty of Chemical and Food Technology, Ho Chi Minh City University of Technology and Education, HCMC, Vietnam

Email: linhnm@hcmute.edu.vn

Check for updates

VNUHCM PRESS

ABSTRACT

This study fabricated chitosan beads obtained from pineapple peels as sustainable biosorbents for hexavalent chromium (Cr (VI)) extraction from water, thus supporting circular economy initiatives. Heavy metal pollution in water systems is a crucial environmental issue that has serious consequences for human health, aquatic ecosystems, and the overall environment. Heavy metals such as lead (Pb), cadmium (Cd), chromium (Cr), zinc (Zn), and copper (Cu) are particularly problematic since they are non-biodegradable, tend to bioaccumulate in organisms, and have the ability to impair cellular function, posing long-term ecological and public health problems. Two biosorbents, PPA (glutaraldehyde crosslinked) and PPB (citric acid crosslinked), were synthesized and investigated using SEM and FTIR to investigate the structural and functional changes caused by the crosslinking agents. While PPB included more carboxyl groups due to citric acid crosslinking, FTIR analysis confirmed the presence of functional groups required for Cr (VI) binding. With optimal Cr (VI) removal at pH 3.0, testing results revealed maximal adsorption capacities of 18.87 mg/g for PPA and 21.01 mg/g for PPB. Increased availability of functional groups and adsorption surface stability improve PPB performance. Adsorption isotherm analysis revealed that both biosorbents followed the Freundlich model, indicating a heterogeneous adsorption mechanism. Kinetic investigations identified pseudo-first-order chemisorption as the major mechanism. Thermodynamic investigation revealed negative Gibbs free energy values (ΔG), confirming the spontaneous nature of Cr (VI) adsorption. With PPB showing improved performance, this study demonstrates the efficacy of chitosan beads generated from pineapple peels as a sustainable and low cost biosorbent for heavy metal cleanup. The findings emphasize the importance of crosslinking agents in improving biosorbent performance, giving valuable information for the development of efficient and cost-effective wastewater treatment methods aligned with sustainability and circular economy concepts.

Key words: Pineapple peel, Hexavalent chromium, Agricultural waste, Adsorption, Biosorbent

INTRODUCTION

Heavy metal pollution in water systems is a crucial environmental issue that has serious consequences for human health, aquatic ecosystems, and the overall environment[1]. Heavy metals such as lead (Pb), cadmium (Cd), chromium (Cr), zinc (Zn), and copper (Cu) are particularly problematic since they are non-biodegradable, tend to bioaccumulate in organisms, and have the ability to impair cellular function, posing long-term ecological and public health problems[2]. Prolonged exposure to heavy metals can have a variety of negative health consequences, including neurotoxicity, carcinogenesis, and kidney impairment, emphasizing the critical need for efficient and sustainable technologies to remove these contaminants from water sources[3]. Chemical precipitation, ion exchange, membrane filtration, and electrochemical procedures are some of the traditional heavy metal removal methods[4]. While these methods are efficient, they are frequently associated with considerable disadvantages. Chemical precipitation, for example, produces a substantial volume of sludge that requires additional treatment, whereas ion exchange and membrane filtering are expensive and require continual material maintenance and regeneration[5–7]. Furthermore, the energy-intensive nature of these processes, as well as their potential to emit secondary pollutants, has prompted research into more sustainable alternatives[8].

In recent years, biosorbents—biological materials capable of adsorbing contaminants—have emerged as a promising alternative due to their eco-friendliness, cost-effectiveness, and natural abundance. Plants, fungus, and agricultural waste can all be used to produce biosorbents[9]. Agricultural waste products, such as fruit peels, sawdust, and rice husks, have received

a lot of interest because they are high in cellulose, hemicellulose, lignin, and other components that help heavy metal ions bond together [10,11]. The use of agricultural waste as a feedstock for biosorbents is consistent with circular economy ideas, which involve transforming waste materials into valuable resources for environmental purposes [12]. Pineapple peel is a common agricultural waste that has great potential as a biosorbent. Pineapple peel includes considerable amounts of cellulose, hemicellulose, lignin, and pectin, all of which have natural adsorption properties for metal ions [13]. Chitosan, a biopolymer formed from the deacetylation of chitin, has been extensively researched for its ability to adsorb heavy metals due to the presence of functional groups such as amino (-NH_2) and hydroxyl (-OH) groups that readily bind with metal ions [14]. Chitosan has a strong affinity for metals such as Pb, Cd, and Cu, as evidenced by electrostatic interaction between its amine groups and positively charged metal ions [15]. However, pure chitosan has some drawbacks, such as solubility in acidic solutions and susceptibility to breakdown at high pH levels, limiting its practical use as an adsorbent [16]. This has prompted researchers to investigate crosslinking chitosan with other materials to improve its stability, mechanical strength, and overall adsorption capability.

Crosslinking chitosan with pineapple peel combines the characteristics of both materials, increasing the biosorbent's ability to operate over a wide pH range while maintaining structural integrity and adsorption capacity [17]. Crosslinked chitosan-based biosorbents have been demonstrated to be more resistant to chemical degradation and have better mechanical properties, making them more appropriate for practical water treatment applications [18]. Furthermore, the generation of crosslinked chitosan-pineapple peel biosorbents provides further environmental advantages. By recycling waste materials, the strategy decreases the environmental impact of agricultural waste disposal while also contributing to a closed-loop system that promotes sustainable waste management practices. This is consistent with the broader goals of green chemistry and environmental sustainability, making crosslinked biosorbents a feasible alternative for tackling the global problem of heavy metal pollution in water bodies [19].

In the biosorbents, glutaraldehyde and citric acid work together as crosslinking agents to enhance structural stability and adsorption performance. Glutaraldehyde reacts with hydroxyl (-OH) groups in the pineapple peel and amine (-NH_2) groups in chitosan, forming strong covalent bonds that create a durable,

rigid framework with improved mechanical strength and resistance to degradation [20,21]. On the other hand, citric acid, as a natural and environmentally friendly crosslinker, forms ester bonds with hydroxyl and carboxyl (-COOH) groups, adding more carboxyl groups that serve as active sites for heavy metal ion binding [22]. The combination of glutaraldehyde for durability and citric acid for increasing functional groups results in a robust, highly effective, and sustainable biosorbent capable of removing heavy metals like Cr(VI), Pb(II), and Cu(II) in wastewater treatment [23].

This work aims to create an effective biosorbent by crosslinking agents with pineapple peel -chitosan beads and testing its efficacy in heavy metal adsorption from aqueous solutions. The findings of this study will add to the expanding body of knowledge on sustainable water treatment technologies and provide a scalable solution for the removal of heavy metals from industrial and municipal wastewater.

MATERIALS AND METHODS

Chemicals and Materials

In this study, isopropyl alcohol (C_3H_8O), succinic acid ($C_4H_6O_4$), chitosan, methanol (CH_3OH), citric acid ($C_6H_8O_7$), sulfuric acid (H_2SO_4), sodium hydroxide (NaOH), Glutaraldehyde 2.5 %, and 1,5 Diphenylcarbazide were obtained from Alpha Chemical Reagent Co., Ltd. (Tianjin, China) and qualified as an analytical grade. All working solutions used during all experiments were prepared by diluting chemicals in deionized water.

Preparation of absorbent

Pineapple peel waste was collected and thoroughly washed with water several times to remove dirt. The cleaned material was blended using a 400W blender. As the blended material still retained moisture, it was subsequently dried in an oven at 80 °C for 12 hours to ensure complete dehydration. To prepare biosorbent beads, pineapple powder, chitosan, and 7% acetic acid were mixed in a ratio of 1 g : 10 g : 240 mL in a beaker. The mixture was stirred continuously using a magnetic stirrer for 12 hours. The resulting slurry was degassed under vacuum and then dropwise added into 200 mL of an alkaline coagulating solution composed of distilled water, methanol, and NaOH in a weight ratio of 4:5:1. This process yielded spherical beads with an average diameter of 3.5 mm. The formed beads were collected and thoroughly rinsed with distilled water to remove residual chemicals and achieve neutral pH.

For the preparation of the glutaraldehyde-crosslinked biosorbent (PPA), the beads were soaked in a 2% glutaraldehyde solution for 12 hours, followed by repeated washing with distilled water until a neutral pH was reached. Alternatively, for the citric acid-crosslinked biosorbent (PPB), the beads were soaked in 3% citric acid for 1 hour. After treatment, the beads were washed several times with distilled water until neutral pH was achieved. The final biosorbent beads (PPA and PPB) were stored in a cool, dry environment to prevent moisture absorption before being used in metal ion adsorption experiments.

Batch experiment

Biosorption experiments were conducted using a batch experiment. All experiments were performed in duplicate by mixing 2 g/L of the biosorbents (PPA or PPB) with 100 mL of Cr(VI) solution at an initial concentration of 25 mg/L. The mixtures were agitated in an orbital shaker incubator at 200 rpm and 303 K. After equilibration, the solutions were filtered, and the residual Cr(VI) concentrations were determined using the diphenylcarbazide method.

The effect of agitation time on Cr(VI) removal was evaluated at 303 K and 200 rpm using 2 g/L of biosorbent. The influence of adsorbent dosage was also investigated, ranging from 0.5 to 5 g/L, to determine the optimal amount for maximum Cr(VI) uptake. The effect of pH on biosorption was examined across a pH range of 2.0–7.0, adjusted using appropriate buffer solutions. Additionally, the impact of temperature was studied over the range of 303–318 K under optimal agitation time and pH conditions.

$$q_e = \frac{(C_0 - C_e) \times V}{m} \qquad (1)$$

where: C_e (mg/L) is the Cr(VI) concentration at equilibrium; C_0 (mg/L) is the initial concentration of Cr(VI); q_e (mg/g) is the adsorption capacity at equilibrium; V (L) is the volume of Cr(VI) solution; m (g) is the mass of the adsorbent.

Absorbent characterization

Their surface morphology was displayed using scanning electron microscope (SEM) images (JSM-6510 LV; Japan). Fourier-transform infrared spectroscopy (FTIR; FT/IR-4600; Japan) determined the main functional groups on their surface.

Adsorption kinetics

The experiments were carried out to investigate the kinetics of heavy metal ions adsorption. Kinetic parameters were studied using the pseudo-first-order (PFO) model, and the pseudo-second-order (PSO) model[24].

The PFO and PSO models were as follows by equations (2) and (3):

$$q_t = q_e(1 - e^{-k_1 t}) \qquad (2)$$

$$q_t = \frac{q_e^2 k_2 t}{1 + k_2 q_e} \qquad (3)$$

where: q_t (mg/g): The adsorption capacity at time, k_1, k_2: The pseudo-first order and pseudo-second order kinetic rate constant.

The intra-particle diffusion model predicts whether there is any resistance during adsorption reaction due to intraparticle diffusion[25], equation (4):

$$q_t = k_i t^{0.5} + C \qquad (4)$$

where k_i is the intraparticle diffusion rate constant (g/mg min$^{0.5}$), and C is the intercept that signifies the boundary layer effect. When the intercept has a larger value, the boundary layer effect is greater, contributing most to the resistance on the surface adsorption process.

Adsorption isotherms

According to the Langmuir model, the adsorbate forms a monolayer on the adsorbent's surface. Equation (5) describes the Langmuir isotherm model.

$$q_e = \frac{q_{max} K_L C_e}{1 + K_L C_e} \qquad (5)$$

Where:

q_{max} (mg/g): The maximum adsorption capacity, K_L (L/mg): The Langmuir constant.

The Freundlich model suggests multilayer adsorption and depends on the assumption that adsorbed molecules interact. The Freundlich isotherm is defined by equation (6)[26].

$$q_e = K_F C_e^{1/n} \qquad (6)$$

Where:

n: The adsorption intensity,

K_F: The Freundlich constant.

The Redlich-Peterson isotherm was developed to rectify the limitations of the Freundlich and Langmuir isotherms. This model combines aspects of the Freundlich and Langmuir models, potentially demonstrating adsorption equilibrium across a wide range of adsorbate concentrations. The nonlinear representation of this data model is delineated by Equation (7).

$$q_e = \frac{K_{RP} C_e}{1 + a_{RP} C_e^g} \qquad (7)$$

Where:

K_{RP} (L/g) and a_{RP} (mg/L)$^{-g}$: the Redlich–Peterson constants; g: an exponent whose value must lie between 0 and 1.

The Temkin isotherm suggests that the heat of adsorption on particle surfaces decreases linearly rather than logarithmically. Furthermore, it is thought that the binding energies involved in the adsorption reaction are uniformly distributed over the adsorbent's surface[27]. The following equation (8) provides the model.

$$q_e = \frac{R \times T}{b} \times lnA_T + \frac{R \times T}{b} \times lnC_e \qquad (8)$$

where A_T is expressed as Temkin isotherm equilibrium binding constant (L/g), b (J/mol) is the constant related to the heat of the adsorption, R is the universal gas constant (8.314 J/mol/K), and T is the temperature (K).

Thermodynamic study

The thermodynamic parameters (DG^o, DH^o, and DS^o) were calculated to examine phosphate adsorption on the adsorbents mentioned above. The Gibbs free energy (G°) of adsorption was calculated as follows from (9) to (12)[28].

$$\triangle G = -RT lnK_c \qquad (9)$$

The following describes the relationship of DG^o to DH^o and DS^o:

$$\triangle G^\circ = \triangle H^\circ - T \triangle S^\circ \qquad (10)$$

$$lnK_c = \frac{-H^o}{R} \times \frac{1}{T} + \frac{S^o}{R} \qquad (11)$$

$$K_C = \frac{MW \times 1000 \times K_L}{\gamma} \qquad (12)$$

where:

K_c: the equilibrium constant; K_L: Langmuir constant (L/mg); MW: molecular mass of the pollutant (g/mol).

RESULTS AND DISCUSSION

Absorbent characterization

The SEM images provide clear evidence of morphological changes in the biosorbents PPA and PPB before and after Cr (VI) adsorption. The PPA surface prior to adsorption (Figure 1, a) appears rough, porous, and heterogeneous with layered and cracked structures, indicating a high surface area favorable for adsorption. After Cr (VI) adsorption (Figure 1, b), the PPA surface becomes noticeably smoother, with visible pore blockage and flake-like deposits, suggesting that Cr(VI) ions were successfully adsorbed onto and partially filled the surface cavities. In contrast, the PPB biosorbent exhibits a relatively smooth and compact surface before adsorption (Figure 1, c), consistent with the effect of citric acid crosslinking, which may have contributed to a more uniform surface structure. The following adsorption (Figure 1, d), significant surface deformation, cracks, and particle deposition are observed on PPB, indicating a strong interaction between Cr(VI) and the carboxyl-rich surface. These morphological changes confirm that both biosorbents effectively adsorbed Cr(VI), with PPB showing more pronounced surface modifications, supporting its higher adsorption performance.

Figure 1 (e) and (f) showed the FTIR analysis of both PPA and PPB biosorbents before and after Cr(VI) adsorption and revealed significant spectral changes, confirming the involvement of functional groups in metal binding. A broad band around 3400 cm^{-1} corresponding to –OH and –NH stretching was observed to shift and intensify after adsorption, suggesting hydrogen bonding and possible coordination with Cr(VI). In both spectra, peaks around 1600–1700 cm^{-1} (attributed to C=O or N–H bending) also showed noticeable shifts, indicating the participation of carbonyl or amine groups in the adsorption process. Additionally, alterations in the 1000–1300 cm^{-1} region, associated with C–O and C–N stretching, further support the chemical interaction between Cr(VI) and the biosorbent surface. These changes collectively demonstrate that hydroxyl, amino, and carboxyl functional groups play key roles in Cr(VI) biosorption for both glutaraldehyde-crosslinked PPA and citric acid-crosslinked PPB materials.

Effect of pH on adsorbents

pH is crucial in all adsorption studies, and even minor changes in solution pH can greatly improve adsorbent efficiency (Figure 2). The current investigation focused on pH levels ranging from 2 to 7. pH changes were conducted with 0.1 M H_2SO_4 and 0.1 M NaOH.Figure 2 shows the observed variations in removal effectiveness as a function of pH. As the pH increased from 2 to 7, Cr (VI) removal effectiveness decreased from 39.5% to 1.0% for PPA material and 67.4% to 41.4% for PPB material. The results demonstrate that eliminating Cr (VI) in an aqueous solution works better at lower pH. The increased removal efficacy of Cr (VI) under acidic conditions could be attributed to charge density. At lower pH, Cr (VI) exhibits a large negative charge density due to the existence of ions like $HCrO_4^-$, $Cr_2O_7^{2-}$, and CrO_4^{2-}
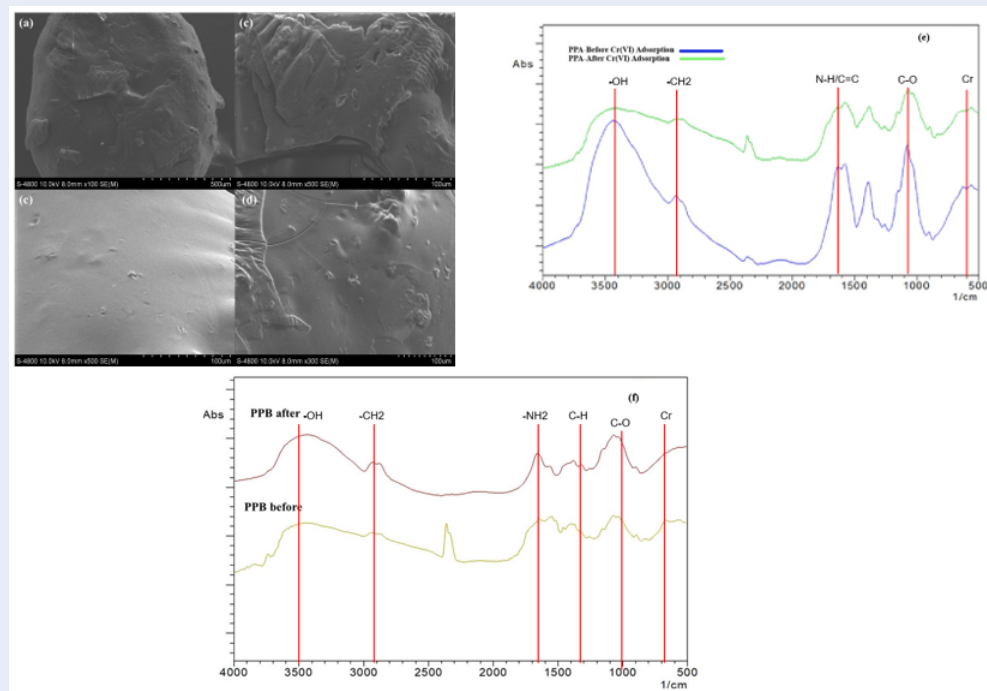
Figure 1: SEM images of PPA (a, b) and PPB (c,d) materials; Before and After Cr(VI) adsorption; (e) FITR spectra of PPA material before and after Cr(VI) adsorption; (f) FITR spectra of PPB material before and after Cr(VI) adsorption.

in the solution [29]. Because of the large concentration of H^+ ions on the adsorbent surface, these ionic forms preferentially adhere there. Adsorbent positively charged surfaces exhibit high electrostatic attraction with Cr (VI) ions [30]. As the pH increases, the interaction between the anionic species and the adsorbent surface diminishes for two primary reasons: (a) the adsorbent surface acquires a negative charge at elevated pH levels, and (b) there is an increase in hydroxyl ions in the aqueous solution [31]. The electrostatic interaction between oppositely charged metal ions and the adsorbent's surface diminishes, resulting in reduced removal of Cr (VI) ions.

Effect of contacting time and adsorbents 'dosage on Cr(VI) removal capacity

In general, removal efficiency improves with increased contact duration.Figure 3 shows the percentage removal of Cr (VI) as a function of time. It was discovered that when the contact time rose from 0 to 480 minutes, more Cr (VI) ions were eliminated. After 480 minutes, there was no obvious increase in Cr (VI) removal. Due to the instantaneous sorption of metal ions on active binding sites that are more numerous on the adsorbent's outer surface, the initial rate of Cr (VI) adsorption was observed to be higher.
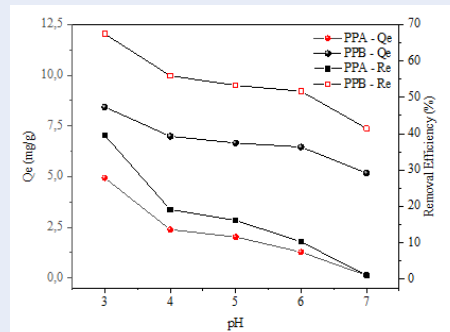

Figure 2: Effect of pH on Adsorption Capacity (Qe) and Removal Efficiency (Re) of PPA and PPB Adsorbents

At the end of the process, there is no visible change in the rate of adsorption and removal because metal ions gradually enter the adsorbent's internal pore structures as the contact length increases, further blocking the active binding sites [32].

Figure 4 shows the results of effect of adsorbent dose on adsorption capacity (Qe) and removal efficiency (Re) of PPA and PPB adsorbents. In metal removal investigations, the adsorbent dosage is crucial. In batch studies, the adsorbent dosage ranged from 0.5 to 5
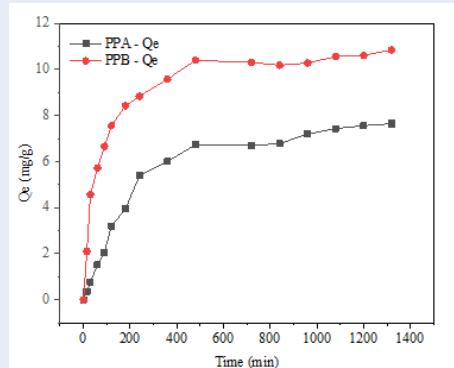
Figure 3: Effect of contact time on Adsorption Capacity (Qe) of PPA and PPB Adsorbents
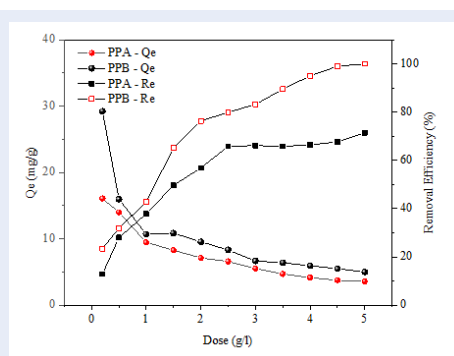

Figure 4: Effect of adsorbent dose on Adsorption Capacity (Qe) and Removal Efficiency (Re) of PPA and PPB Adsorbents

g/L. The results indicated that the removal efficiency of Cr (VI) increased with the adsorbent dosage; for example, 0.5 g/L of Cr (VI) removed 27.9% of the material for PPA and 31.9% of the material for PPB within 480 minutes, while 5 g/L removed all of the Cr (VI) within 480 minutes, indicating 100% removal (Figure 4). This could be because a higher adsorbent dosage will have more surface area, which will bind more metal ions [33]. After all, the adsorption process will have many new binding sites accessible, preferring a high rate of adsorption.

Adsorption kinetics, isotherms and thermodynamics

The kinetic analysis of heavy metal adsorption onto biosorbents (PPA and PPB) provides valuable insights into the adsorption mechanisms and efficiency of these materials. The study utilized three widely accepted kinetic models—pseudo-first order (PFO), pseudo-second-order (PSO), and intra-particle diffusion models—to interpret the adsorption behavior observed experimentally.

The parameters and correlation coefficients (R^2) for the kinetic models are presented in Table 1. For the PPA biosorbent, R^2 values ranging from 0.91 to 0.99 indicate that the pseudo-first order (PFO) model is applicable compared to other kinetic models. This implies that the adsorption process is predominantly governed by physical adsorption mechanisms, such as weak Van der Waals forces. However, the possibility of chemical adsorption cannot be excluded, as suggested by the high correlation coefficient ($R^2 = 0.98$), which points to interactions between heavy metal ions and functional groups on the chitosan and pineapple peel matrix via electron sharing or exchange. On the other hand, the pseudo-second order (PSO) model demonstrated the best fit for the PPB biosorbent, with an adjusted R^2 value of 0.98. This indicates that chemisorption is the dominant mechanism, involving strong chemical interactions such as ion exchange or complexation between heavy metals and the active sites on the biosorbent. Additionally, as the concentration of Cr(VI) ions increased, the adsorption capacity rose while the rate constant decreased. This behavior can be explained by the reduced competition for active sites at lower concentrations, whereas at higher concentrations, the competition for these sites became significantly more intense. Identifying the rate-limiting steps for the adsorption of Cr(VI) ions on PPA and PPB required a thorough understanding of the adsorption mechanism, which was not adequately explained by pseudo-first order and pseudo-second-order kinetic models. The intraparticle diffusion model was employed to elucidate the diffusion mechanism. The results from the intraparticle diffusion model for PPA and PPB reveal significant differences in their adsorption mechanisms. For PPA, the model showed a high R^2 value of 0.91 indicating that, while pore diffusion is important, surface adsorption or external mass transfer also contributes, especially in the initial stages. This suggests that PPA's relatively uniform structure, due to crosslinking, facilitates the effective diffusion of Cr(VI) ions into its pores. In contrast, PPB exhibited a lower R^2 value of 0.76, indicating that intraparticle diffusion is less significant in its adsorption process. While the Ki value of 0.24 indicates faster pore diffusion to a more dominant surface adsorption mechanism in the early stages. This can be attributed to the more heterogeneous surface of PPB, which likely limits the contribution of intraparticle diffusion. Overall, PPA relies more on both surface interactions and pore diffusion

due to its homogeneous structure, while PPB's adsorption is largely driven by surface interactions, reflecting its more varied surface characteristics.

Table 1: Kinetic parameters of adsorbent materials for Cr(VI) adsorption

	Units	PPA	PPB
1. PFO model			
Q_e	mg/g	7.4	12.2
K_1	min-1	0.0045	0.0125
Adj-R^2	-	0.99	0.97
2. PSO model			
Q_e	mg/g	8.98	11.1
K_2	g/mg.min	0.0005	0.002
Adj-R^2	-	0.98	0.99
3. Intra particle diffusion			
K_i	mg/(g min1/2)	0.23	0.24
Adj-R^2	-	0.91	0.76

The adsorption isotherm analysis of pineapple peel crosslinked chitosan biosorbents, PPA and PPB, provides insight into their adsorption mechanisms and capacity for heavy metal removal. Both biosorbents were evaluated using the Langmuir, Freundlich, Temkin, and Redlich-Peterson models, which allowed us to assess their adsorption performance and determine the nature of the adsorption interactions. Table 2 shows the R^2 value and extra coefficients from the nonlinear regression study. The isotherm models were sorted based on R^2 values, with the best-fitting model discovered first. The models are arranged as follows: Freundlich, Langmuir, Redlich-Peterson, and Temkin. The Freundlich value "n" ranges from 0 to 10, indicating that the adsorption of Cr(VI) ions onto PPA and PPB is physical in nature. The results showed that the Freundlich model fit the adsorption equilibrium data better than the other isotherm models. This suggests that Cr(VI) ions are adsorbed onto biosorbents in a heterogeneous, multilayered way. The Langmuir maximum monolayer adsorption capacities of the PPA and PPB adsorbents were determined to be 18.87 mg/g and 20.37 mg/g, respectively. The Temkin model predicts that the heat of adsorption values for the current adsorption system are less than 8 kJ/mol, indicating a weak interaction between the adsorbent and Cr(VI) ions. This suggests that the current adsorption method relies on

physical adsorption. The Redlich-Peterson isotherm shows that PPA and PPB have βRP values of 0.64 and 0.72, respectively. "βRP" refers to an exponent between 0 and 1. This section explains the relevance of βRP. When βRP = 0, the Redlich-Peterson equation simplifies to Henry's law, while βRP = 1 corresponds to the Langmuir equation. The Redlich-Peterson equation can be understood as being consistent with Henry's law for low Cr(VI) ion concentrations and with the Freundlich isotherm model at higher values. The isotherm data indicate that the Freundlich isotherm model best describes the current adsorption system, as demonstrated by a greater correlation coefficient and lower error values.

Table 2: Isotherm parameters of adsorbent materials for Cr(VI) adsorption

	Units	PPA	PPB
1. Langmuir model			
Q_{max}	mg/g	18.87	20.37
K_L	L/mg	0.0012	0.0035
Adj-R^2	-	0.97	0.84
2. Freundlich model			
K_F	(mg/g)/(mg	0.18	0.004
n	-	0.78	0.51
Adj-R^2	-	0.99	0.99
3. Redlich-Peterson model			
K_{RP}	L/mg	1.271	1.916
α_{KP}	$(mg/L)^{-g}$	1.785	6.552
β_{KP}	-	0.64	0.72
Adj-R^2	-	0.96	0.76
4. Temkin model			
A_T	L/g	0.067	0.057
B	-	37.38	26.07
b	J/mol	69.62	99.82
Adj-R^2	-	0.81	0.64

Thermodynamic parameters for the adsorption of Cr(VI) by PPA and PPB at varying temperatures are shown in Table 3. At every temperature, both materials show negative Gibbs free energy ($\Delta G°$) values, suggesting that the adsorption process is spontaneous[34]. PPB has a similar tendency, with $\Delta G°$ falling from -73.76 kJ/mol to -79.04 kJ/mol over the same temperature range, whereas PPA's declines from -72.38 kJ/mol at 303 K to -78.18 kJ/mol at 318 K. This implies

that both materials benefit from the adsorption process at higher temperatures. The endothermic process is indicated by the enthalpy change ($\Delta H°$) of 44.41 kJ/mol for PPA and 33.09 kJ/mol for PPB, which is also endothermic but to a lesser extent [35]. With PPA at 387.96 J/mol·K and PPB at 352.71 J/mol·K, the entropy change ($\Delta S°$) is positive for both materials, indicating greater randomness at the solid-liquid interface during adsorption [36]. This can be explained by the fact that water molecules that are displaced by adsorbents gain more entropy than those that are lost due to $HCrO_4^-$ anions dissociating. These findings demonstrate how well both materials work for Cr(VI) adsorption, with PPB performing somewhat better at higher temperatures.

Table 3: Thermodynamic parameters of adsorbent materials for Cr(VI) adsorption

Materials	Temperature (K)	ΔG^o (kJ/mol)	ΔH^o (kJ/mol)	ΔS^o (J/mol.K)
PPA	303	-72.38	44.41	387.96
	313	-76.3		
	318	-78.18		
PPB	303	-73.76	33.09	352.71
	313	-77.33		
	318	-79.04		

CONCLUSIONS

According to the study's findings, PPA and PPB materials show great promise as biosorbents, with both being particularly effective at removing Cr(VI) from aqueous solutions. It was observed that the optimal pH for Cr(VI) biosorption on these materials was 3.0, which corresponds to the conditions that allow for the highest adsorption efficiency. PPB was the most effective adsorbent of the materials tested, with an even higher capacity of 21.01 mg/g at 303 K than PPA compounds, particularly PPA, which had an adsorption capacity of 18.87 mg/g. The Freundlich isotherm model fit the experimental data well, demonstrating the diversity of adsorption sites on different biosorbents. Physical sorption may be the rate-limiting step, as kinetic experiments revealed that the adsorption process followed the pseudo-first-order model. The biosorption process was endothermic and spontaneous, as evidenced by negative ΔG values for Cr(VI) uptake and positive ΔH values for heat absorption during adsorption (thermodynamic analysis). Thus, PPA and PPB materials have considerable promise for real-world applications in removing heavy metals from contaminated water sources, especially when crosslinked with citric acid.

ACKNOWLEDGEMENTS

COMPETING INTERESTS

The author declares that they have no conflict of interest.

AUTHORS' CONTRIBUTIONS

Nguyen My Linh: Supervision, Writing - original draft, reviewing and Editing; Data curation, Formal analysis; Methodology, Conceptualization.

REFERENCES

1. Mishra S, et al. Heavy metal contamination: an alarming threat to environment and human health. Environmental biotechnology: For sustainable future. 2019;p. 103–125.
2. Kanwar VS, et al. Phytoremediation of toxic metals present in soil and water environment: a critical review. Environmental Science Pollution Research. 2020;27:44835–44860.
3. Parida L, Patel TN. Systemic impact of heavy metals and their role in cancer development: a review. Environmental Monitoring Assessment. 2023;195(6):766.
4. Peng H, Guo JJECL. Removal of chromium from wastewater by membrane filtration, chemical precipitation, ion exchange, adsorption electrocoagulation, electrochemical reduction, electrodialysis, electrodeionization, photocatalysis and nanotechnology: a review. Environmental Chemistry Letters. 2020;18(6):2055–2068.
5. Saleh TA, Mustaqeem M, Khaled M. Water treatment technologies in removing heavy metal ions from wastewater: A review. Environmental Nanotechnology, Monitoring Management. 2022;17:100617.
6. Rezai B, Allahkarami E. Wastewater treatment processes—techniques, technologies, challenges faced, and alternative solutions. Soft computing techniques in solid waste and wastewater management. 2021;p. 35–53.
7. Shrestha R, et al. Technological trends in heavy metals removal from industrial wastewater: A review. Journal of Environmental Chemical Engineering. 2021;9(4):105688.
8. Ma Q, et al. Transition Metal Catalysts for Atmospheric Heavy Metal Removal: A Review of Current Innovations and Advances. Molecules. 2023;28(22):7620.
9. Karić N, et al. Bio-waste valorisation: Agricultural wastes as biosorbents for removal of (in) organic pollutants in wastewater treatment. Chemical Engineering Journal Advances. 2022;9:100239.
10. Alalwan HA, Kadhom MA, Alminshid AH. Removal of heavy metals from wastewater using agricultural byproducts. Journal of Water Supply: Research Technology—AQUA. 2020;69(2):99–112.
11. Younas F, et al. A critical review on the separation of heavy metal (loid) s from the contaminated water using various agricultural wastes. International journal of phytoremediation. 2024;26(3):349–368.
12. Madeła M, Skuza M. Towards a circular economy: analysis of the use of biowaste as biosorbent for the removal of heavy metals. Energies. 2021;14(17):5427.
13. Rosales E, et al. Sustainable removal of Cr (VI) by lime peel and pineapple core wastes. Applied Sciences. 2019;9(10):1967.

14. Sarode S, et al. Overview of wastewater treatment methods with special focus on biopolymer chitin-chitosan. International journal of biological macromolecules. 2019;121:1086–1100.

15. Zhang Y, et al. Research progress of adsorption and removal of heavy metals by chitosan and its derivatives: A review. Chemosphere. 2021;279:130927.

16. Upadhyay U, et al. Recent advances in heavy metal removal by chitosan based adsorbents. Carbohydrate Polymers. 2021;251:117000.

17. Brião G, et al. Removal of toxic metals from water using chitosan-based magnetic adsorbents. A review. Environmental Chemistry Letters. 2020;18:1145–1168.

18. Bhatt P, et al. Developments and application of chitosan-based adsorbents for wastewater treatments. Environmental Research. 2023;226:115530.

19. Nawaz S. Effective assessment of biopolymer-based multifunctional sorbents for the remediation of environmentally hazardous contaminants from aqueous solutions. Chemosphere. 2023;329:138552.

20. Bilal M, et al. Immobilized lipases-based nano-biocatalytic systems—A versatile platform with incredible biotechnological potential. International Journal of Biological Macromolecules. 2021;175:108–122.

21. Nguyen ML, Juang RS. Modification of crosslinked chitosan beads with histidine and Saccharomyces cerevisiae for enhanced Ni(II) biosorption. Journal of the Taiwan Institute of Chemical Engineers. 2015;56:96–102.

22. He Y, et al. Citric acid cross-linked β-cyclodextrins: A review of preparation and environmental/biomedical application. Carbohydrate Polymers. 2024;323:121438.

23. Keirudin AA, Zainuddin N, Yusof NA. Crosslinked carboxymethyl sago starch/citric acid hydrogel for sorption of Pb2+, Cu2+, Ni2+ and Zn2+ from aqueous solution. Polymers. 2020;12(11):2465.

24. Revellame ED, et al. Adsorption kinetic modeling using pseudo-first order and pseudo-second order rate laws: A review. Cleaner Engineering Technology. 2020;1:100032.

25. Wang J, Guo X. Rethinking of the intraparticle diffusion adsorption kinetics model: Interpretation, solving methods and applications. Chemosphere. 2022;309:136732.

26. Lima EC, Adebayo MA, Machado FM. Kinetic and equilibrium models of adsorption. Carbon nanomaterials as adsorbents for environmental biological applications. 2015;p. 33–69.

27. Travin S, et al. Kinetic simulation of adsorption isotherms. Russian Journal of Physical Chemistry B. 2019;13:975–985.

28. Dat ND, et al. Performance of heterogeneous Fenton catalyst from solid wastes for removal of emerging contaminant in water: a potential approach to circular economy. Results in Engineering. 2023;18:101086.

29. Kumari A, Sinha A, Singh D. Iron-Based Modified Nanomaterials for the Efficacious Treatment of Cr (VI) Containing Wastewater: A Review. Persistent Pollutants in Water Advanced Treatment Technology. 2023;p. 299–331.

30. Zhang Y, et al. Effects of ionic strength on removal of toxic pollutants from aqueous media with multifarious adsorbents: A review. Science of the Total Environment. 2019;646:265–279.

31. John Y, David VE, Mmereki D. A comparative study on removal of hazardous anions from water by adsorption: a review. International Journal of Chemical Engineering. 2018;(1):3975948.

32. Chen S, et al. Equilibrium and kinetic adsorption study of the adsorptive removal of Cr (VI) using modified wheat residue. Journal of colloid interface science. 2010;349(1):256–264.

33. Chakraborty R, et al. Adsorption of heavy metal ions by various low-cost adsorbents: a review. International Journal of Environmental Analytical Chemistry. 2022;102(2):342–379.

34. Bhattacharya A, et al. Adsorption, kinetics and equilibrium studies on removal of Cr (VI) from aqueous solutions using different low-cost adsorbents. Chemical engineering journal. 2008;137(3):529–541.

35. Chen S, et al. Removal of Cr (VI) from aqueous solution using modified corn stalks: Characteristic, equilibrium, kinetic and thermodynamic study. Chemical Engineering Journal. 2011;168(2):909–917.

36. Montoya T, et al. A novel solid–liquid equilibrium model for describing the adsorption of associating asphaltene molecules onto solid surfaces based on the "chemical theory". Energy Fuels. 2014;28(8):4963–4975.

Bài nghiên cứu

Ứng dụng vỏ dứa kết hợp với chitosan làm vật liệu hấp phụ thân thiện với môi trường để loại bỏ kim loại nặng: Hướng tới kinh tế tuần hoàn

Nguyễn Mỹ Linh[*]

Use your smartphone to scan this QR code and download this article

Khoa Công nghệ Hóa học & Thực phẩm, Trường Đại học Sư phạm kỹ thuật TP.HCM , TP. Hồ Chí Minh, Việt Nam

Liên hệ

Nguyễn Mỹ Linh, Khoa Công nghệ Hóa học & Thực phẩm, Trường Đại học Sư phạm kỹ thuật TP.HCM , TP. Hồ Chí Minh, Việt Nam

Email: linhnm@hcmute.edu.vn

Check for updates

VNUHCM PRESS

TÓM TẮT

Nghiên cứu này đã tiến hành điều chế các hạt chitosan kết hợp với sinh khối từ vỏ dứa nhằm tạo ra vật liệu hấp phụ bền vững để loại bỏ Cr(VI) trong nước, góp phần thúc đẩy các sáng kiến về kinh tế tuần hoàn. Ô nhiễm kim loại nặng trong hệ thống nước là một vấn đề môi trường cấp bách, gây ra hậu quả nghiêm trọng đối với sức khỏe con người, hệ sinh thái thủy sinh và môi trường tổng thể. Các kim loại nặng như chì (Pb), cadmi (Cd), crom (Cr), kẽm (Zn) và đồng (Cu) đặc biệt gây lo ngại do chúng không phân hủy sinh học, có xu hướng tích tụ sinh học trong cơ thể sinh vật và có khả năng làm rối loạn chức năng tế bào, dẫn đến các vấn đề lâu dài về môi trường và sức khỏe cộng đồng. Hai loại vật liệu hấp phụ, gồm PPA (liên kết chéo bằng glutaraldehyde) và PPB (liên kết chéo bằng axit citric), đã được tổng hợp và phân tích bằng các kỹ thuật SEM và FTIR để khảo sát các thay đổi về cấu trúc và chức năng do tác động của các tác nhân liên kết chéo. Phân tích FTIR xác nhận sự hiện diện của các nhóm chức có khả năng tương tác với ion Cr(VI), trong đó PPB thể hiện hàm lượng nhóm carboxyl cao hơn nhờ liên kết chéo bằng axit citric. Tại pH tối ưu 3.0, kết quả hấp phụ cho thấy khả năng loại bỏ Cr(VI) của PPB đạt 21.01 mg/g, cao hơn so với PPA là 18.87 mg/g. Hiệu suất vượt trội của PPB được cho là do sự gia tăng nhóm chức hoạt động và độ ổn định bề mặt hấp phụ. Kết quả đẳng nhiệt hấp phụ phù hợp với mô hình Freundlich, phản ánh bản chất bề mặt hấp phụ không đồng nhất của cả hai vật liệu. Phân tích động học cho thấy quá trình hấp phụ tuân theo mô hình giả bậc nhất, gợi ý rằng hấp phụ vật lý là cơ chế chi phối. Bên cạnh đó, giá trị ΔG âm thu được từ phân tích nhiệt động học đã xác nhận tính tự phát của quá trình hấp phụ Cr(VI). Với hiệu suất được cải thiện rõ rệt, đặc biệt ở vật liệu PPB, nghiên cứu này khẳng định tiềm năng ứng dụng của các hạt chitosan từ vỏ dứa như một vật liệu hấp phụ thân thiện với môi trường, chi phí thấp, hiệu quả trong xử lý kim loại nặng. Những kết quả thu được nhấn mạnh vai trò quan trọng của tác nhân liên kết chéo trong việc nâng cao hiệu suất hấp phụ, đồng thời cung cấp cơ sở khoa học hữu ích cho việc phát triển các giải pháp xử lý nước thải phù hợp với định hướng phát triển bền vững và kinh tế tuần hoàn.

Từ khoá: Vỏ quả dứa, Crom (VI), Rác thải nông nghiệp, Hấp phụ, Chất hấp phụ sinh học.